Electron diffraction studies of laser-pumped molecules. IV. SF_6, experiment, and theory

Lawrence S. Bartell and Michael A. Kacner
Department of Chemistry, University of Michigan, Ann Arbor, Michigan 48109

(Received 7 June 1983; accepted 29 March 1984)

A model of absorption of infrared radiation by supersonic jets proposed in paper III was tested experimentally. New nozzle designs permitted pumping the ν_3 mode of SF_6 at power densities in excess of 10^4 W/cm^2. Vibrational excitation corresponding to the absorption of up to 3.6 photons/molecule was deduced from the increased amplitudes of vibration of the SF, FF_{cis}, and FF_{trans} atom pairs and the lengthening of the SF bond. At high excitations, electron diffraction intensities were accounted for best if it was assumed that two subsets of molecules were produced, one much hotter than the other. Vibration–vibration relaxation from ν_3 to the other stretching modes was too fast to be followed. Relaxation of stretching to bending could be monitored, crudely, at lower pressures where approximately 30 collisions were needed at the depressed temperatures in the jet. At higher pressures and excitations V-T/R relaxation was observed, corresponding to a transfer of perhaps one-tenth of the vibrational excitation in the course of 10^3 collisions. Excitation as a function of gas density, power density, and nozzle diameter was accounted for satisfactorily by the model of paper III.

I. INTRODUCTION

Recent research[1–5] has demonstrated the feasibility of generating vibrationally excited molecular beams by pumping supersonic microjets. Advantages and limitations of measuring the excitation by electron diffraction have been discussed in some detail elsewhere.[4,5] Experiments reported to date, proceeding by trial and error, have provided clues helpful in the formulation of a model of the kinetics of excitation. This model, described elsewhere,[6,7] was able to account semiquantitatively for published results[2–5] found at modest cw power densities under a limited range of conditions. It seemed worthwhile to carry out further experiments, both to test the validity of the model and to remedy certain defects in the original experiments. Of particular interest was the investigation of pumping under more extreme conditions. Results of such experiments are described in the following.

II. EXPERIMENTAL

A. Apparatus and conditions

Except where mentioned to the contrary, the diffraction apparatus and tunable cw CO_2 laser were arranged and operated as described previously.[4,5] Power densities ranged up to 10^4 W/cm^2. Gas pressure fell precipitously from values of 20 to 400 Torr at the nozzle tip, passing through values tenfold lower in the first 0.5 μs of expansion. One source of trouble in initial experiments had been the susceptibility of the nozzle (hereafter referred to as nozzle 1) to thermal heating by the laser beam which grazed it during irradiation of the sample. In fact, although thermal excitation was generally small compared with optical pumping, the largest uncertainty in interpreting experiments seems to have been in the somewhat erratic control over the exact fraction of the excitation due to thermal heating. To remove this imperfection two new nozzles were fabricated, one (nozzle 2) with internal dimensions nearly the same as those of nozzle 1 and another (nozzle 3) of larger bore for testing model predictions. Nozzle 2 was made from a hypodermic needle cut to the desired length after being imbedded in a massive coating of silver solder. Nozzle 3 was formed from a block of solid brass. Both nozzles were given a high polish to reflect radiation, and equipped with thermocouples just to the lee side of the nozzle aperture. The mirror finish together with the considerably greater heat capacity and heat conduction than possessed by nozzle 1 was effective in reducing thermal heating to negligible values during typical irradiation times, even when the laser beam was played directly over the exterior of the nozzle.

Because of the more robust character of nozzles 2 and 3 it became feasible to subject the effluent gas to the full power density of the focused radiation. In prior studies it had been necessary to aim the laser beam away from the nozzle by a margin that reduced the power density at the tip by an order of magnitude.

With the new, well-polished and massive nozzles no vestige of the gas outlet could be seen through the alignment collimator-microscope. Therefore, to facilitate centering of the laser beam on the jet axis, provision was made for measuring the attenuation of the laser radiation by absorption by the gas jet and for observing increased gas pressure associated with the decreased efficiency of condensation of SF_6 vapor on a liquid nitrogen trap when the molecules were vibrationally excited. It turned out that the latter method, easily followed by an ionization gauge in the diffraction chamber, gave the most sensitive indication of optimum alignment.

Diffraction patterns of SF_6 were taken as described previously either without radiation (to provide control plates for a given sample pressure) or during irradiation of the sample at laser powers ranging from 5 to 40 W and frequencies from 932 to 1050 cm^{-1}. Power densities produced at the focus of a ZnSe lens (12.7 cm focal length) are discussed later. Conditions under which the diffraction patterns were recorded are listed in Table I and documented in more detail in supplementary data which includes experimental intensities and other pertinent information.[8] Runs with nozzle 1 are those treated in paper II.[5]

 0021-9606/84/130280-08$02.10

TABLE I. Experimental conditions in diffraction experiments.[a]

Nozzle no. (diam, mm)	1(0.12)	1	1	2(0.12)	2	3(0.36)
Nozzle length, mm	4.0			4.9		3.05
Nozzle to plate, cm	21.182	21.116	21.180	21.111	21.131	21.074
Nozzle to el. beam, mm	0.66	0.62	0.52	0.74	0.69	0.46
Nozzle to laser focus, mm	0.3	0.3	0.3	0.35–0.40	0.35–0.40	0.1
Stagnation press, Torr	50–300	80–300	300–600	100–1200	600–1200	30–60
Exposure time, s	10.0–1.5	7.0–1.5	2.0–0.7	10.0–0.6	1.5–0.6	3.0–1.5
Beam current, μA	0.70	0.70	0.70	0.35	0.30	0.36
Number of plates	55	25	145	125	45	10

[a] Sector r^3, 4.8 cm radius, accelerating voltage 40.0 kV.

B. Analysis of diffraction intensities

Analyses were carried out in much the same way as described in detail elsewhere[4,5] with several minor exceptions. First, a more satisfactory emulsion calibration function was employed.[7] Secondly, control plates (whose systematic intensity residuals were used to correct intensities of irradiated samples[4]) were constrained in least squares analyses to incorporate the theoretical shrinkages of Cyvin[9] and amplitudes of vibration of 0.043, 0.061, and 0.054 Å, respectively, for SF, FF_{cis}, and FF_{trans} distances. Dynamic corrections were made according to the theory of Miller and Bartell.[10] Lastly, and perhaps most significantly, the asymmetry constant $\hat{a}(FF_c)$ was revised in the light of recent evidence[11] to equal $\hat{a}$(SF) at the same temperature. This new, much larger, value gives an appreciably better account of the data at high excitations than did the prior function. Further details are discussed elsewhere.[7] Model calculations making possible inferences of the V-T/R and V-V relaxation rates from the diffraction intensities are discussed briefly, later.

III. RESULTS

Effects of vibrational excitation could be observed in all molecular parameters, including the SF, FF_{cis}, and FF_{trans} amplitudes of vibration and the mean SF bond length. Except at low sample densities, where V–V relaxation was incomplete, the FF_{cis} amplitude exhibited the largest change when molecules absorbed radiation. Hence, the observed increase in the *cis* amplitude and the mean number of photons absorbed and retained per molecule (as inferred from the *cis* amplitude) are the principal measures of excitation presented in the following.

According to the treatment[6] developed to account for the laser-pumping kinetics, the mean molecular excitation in supersonic jets should depend in characteristic ways upon the laser frequency, power density, and molecular collision frequency. The latter is governed by the gas density distribution which, itself, depends on sample pressure and nozzle design. Measurements of molecular parameters as a function of frequency, with other conditions fixed, are shown in Figs. 1 and 2. Measurements varying the power density at fixed geometry and pressure are plotted in Fig. 3. Measurements varying the gas density at fixed geometry and laser power are presented in Fig. 4. Measurements jointly varying effective gas density and power density are illustrated in Fig. 5. Such a correlated variation was accomplished by recording diffraction patterns at various fixed distances between the focused

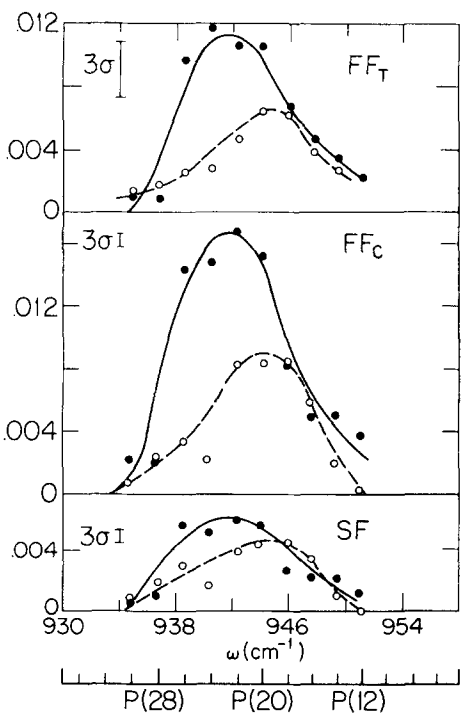

FIG. 1. Observed excitation of SF_6 as a function of incident frequency. Ordinates are the increases in rms amplitude (in Å) of the indicated atom pairs. Experimental conditions for the solid (open) circles corresponding to nozzle 2(1) are approximately $P = 200$ (100) Torr at the nozzle exit and $W \approx 11$ (2) kW/cm^2 at the nozzle tip, neglecting reflection from the nozzle. Data points correspond to a three plate average of the amplitude increase. Error bars show representative uncertainties $3\sigma_{LS}$ for analyses of single plates.

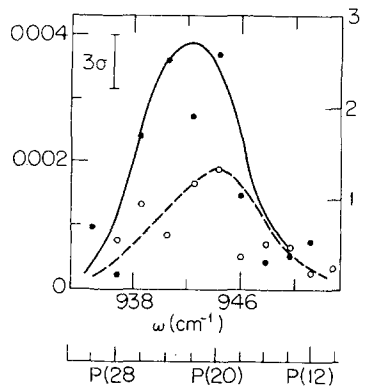

FIG. 2. Solid (open) circles represent the observed optically induced thermal expansion of mean SF bond lengths in SF_6 corresponding to the left-hand scale, in Å, as a function of incident laser frequency for conditions identical to those in Fig. 1. Solid (dashed) curves associated with the right-hand scale are $\langle n \rangle$, the corresponding mean number of photons absorbed per molecule as inferred from FF_{cis} results in Fig. 1. Error bar indicates the single plate uncertainty $3\sigma_{LS}$.

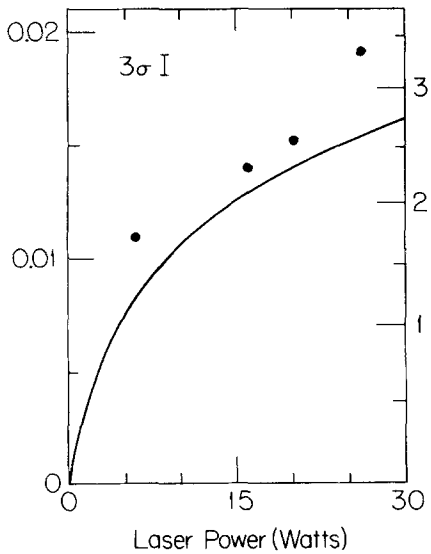

FIG. 3. Excitation of SF_6 by the $P(20)$ line as a function of laser power. Left-hand scale indicates the increase in FF_{cis} amplitude of vibration, in Å, while the right-hand scale shows $\langle n \rangle$. Runs were with nozzle 2 at nozzle tip pressure of 200 Torr, center of focused spot 0.1 mm from nozzle tip. Solid line represents model calculations described in Ref. 6 for the above experimental conditions.

laser spot and nozzle tip. Nozzle 3, threefold larger in bore than nozzle 2, produced a jet absorbing 68% as many photons as one from nozzle 2 when flow rates (0.36 Torr l/s) and irradiation conditions were common [$P(20)$, 20 W, $x_L = 0.1$ mm].

Although trends are reasonably well established there is appreciable scatter in the measurements. The degree to which this is characteristic of the precision in measuring excitation or subject to irreproducibility in experimental conditions is indicated in the error bars in the figures and the data in Fig. 6. Error bars and solid points in Fig. 6 are gauges of the precision of measurement inferred, as discussed in Ref. 5, from least squares analyses of electron intensities. Crosses and open points in Fig. 6 are indices of the variability

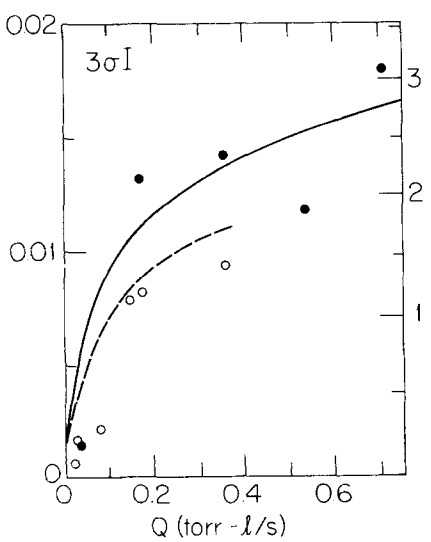

FIG. 4. Excitation of SF_6 as a function of gas throughput for a $P(20)$ line. Solid (open) circles are for gas issuing from nozzle 2(1) with the laser tuned to 20 (30) W and the center of the focused spot 0.1 (0.3) mm from the nozzle tip. Left-hand scale indicates the increase in FF_{cis} amplitude of vibration, in Å, while the right-hand scale represents $\langle n \rangle$. Solid (dashed) lines represent model calculations (Ref. 6).

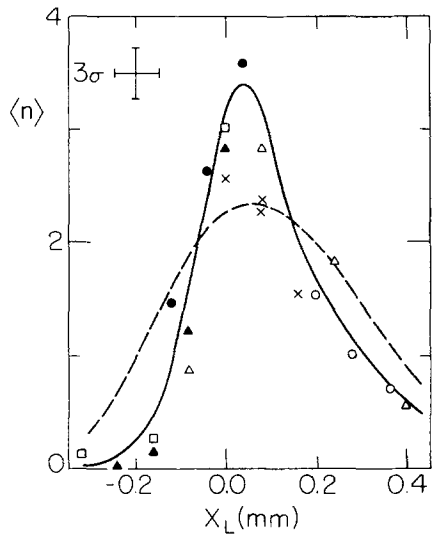

FIG. 5. Plot of $\langle n \rangle$, inferred from FF_{cis} amplitude of vibration, as a function of the distance x_L between the nozzle tip and the center of focused laser beam. Positive distances lie between the nozzle tip and the electron beam. Data from six sets of runs are represented by different symbols. Error bars represent single plate uncertainties $3\sigma_{LS}$. The solid line is a smooth curve drawn through the data points. The dashed curve is calculated by the model of Ref. 6. Runs, with nozzle 2, stagnation pressure 600 Torr, 20 W $P(20)$ line.

of experimental conditions in the runs as well as random errors. One source of variability lay in instabilities of the tuning of the laser leading to fluctuating mode patterns and power densities. Another source was an effect of reflection of radiation from the nozzle that distorted the power density profile as discussed later. Results indicate that the larger excursions of points from smooth trends arose from instabilities in conditions rather than from limitations in the diffraction analysis.

According to the model of paper III,[6] an efficient absorption of radiation requires that T-R and V–V relaxation be fast, and a high retention of vibrational excitation necessitates that V-T/R relaxation be slow. Some information

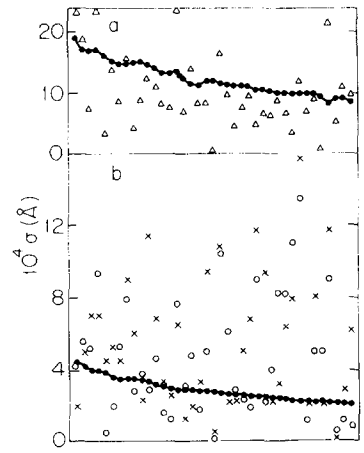

FIG. 6. Two measures of uncertainty in amplitudes of vibration (in Å). Each run of three or four plates (individual points in Figs. 1, 4, and 5) is represented once and plotted, arbitrarily, in order of decreasing σ_{LS} for the FF_{cis} amplitude. Solid points derived from residuals of diffraction intensities are representative single plate σ_{LS} values for the SF and FF_{cis} amplitudes (lower curve, where errors are almost the same for both amplitudes) and for the FF_{trans} amplitude (upper curve). Other symbols represent σ_{rep} a measure of the reproducibility in a given run calculated by Eq. (1), Ref. 5; SF (×), FF_{cis} (○), and FF_{trans} (△).

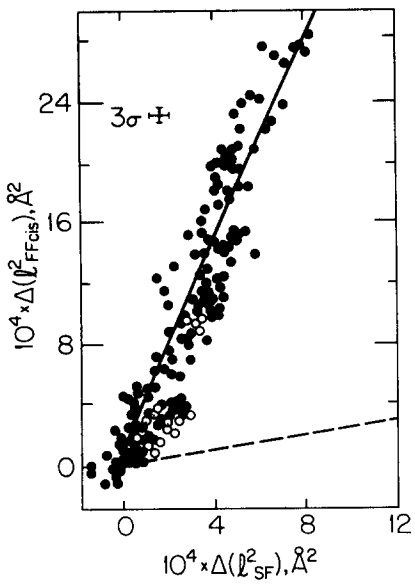

FIG. 7. Evidence of V–V relaxation, from corresponding changes in mean-square amplitudes of FF_{cis} and SF distances. Dashed line calculated for pure ν_3 excitation. Solid line calculated for thermal equilibrium among vibrational modes. Solid circles represent experimental observations for various degrees of pumping of the ν_3 mode under collisional conditions. Open circles are for runs at low collision rate (less than 200 Torr stagnation pressures for nozzles 1 and 2). Error bars are representative single plate uncertainties $3\sigma_{LS}$.

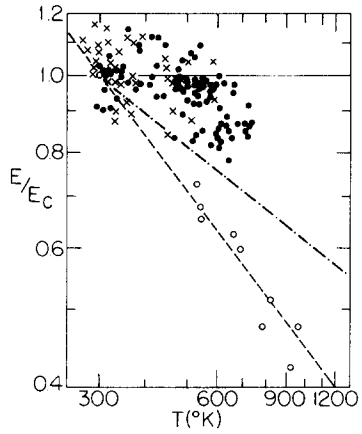

FIG. 9. Evidence of V-T/R relaxation. Relative scattered electron intensities ($E/E_{control}$) as a function of the vibrational temperature T inferred from FF_{cis} amplitudes. Optical excitation experiments with stagnation pressures at or below 300 Torr are represented by crosses and those carried out at or above 600 Torr are represented by solid circles. Points at higher temperature reveal systematic intensity losses associated with gas density attenuation due to translational excitation. Open circles represent effects of thermal excitation from experiments with a heated nozzle (stagnation pressure $\approx$ 300 Torr).

about the latter two relaxation rates is contained in the diffraction intensities. In the 10^{-6} s characteristic time scale of the experiment, excitation in the FF_{cis} vs SF mean square amplitudes as exemplified in Fig. 7 clearly shows a redistribution from the ν_3 pumped mode to a Boltzmann vibrational distribution when stagnation pressures exceed 200 Torr (exit pressures above 70 Torr). At lower pressures, however, V–V relaxation is incomplete. Hence, the distribution of vibrational energy, as deduced from the patterns of amplitude excitation sketched in Fig. 8, departs significantly from that for a Boltzmann distribution. At the highest pressures studied, clear evidence for V-T relaxation can be seen in the diffraction intensity ratios displayed in Fig. 9. These ratios reveal a depletion in gas density at higher excitations due to the release of heat in V-T/R relaxation.

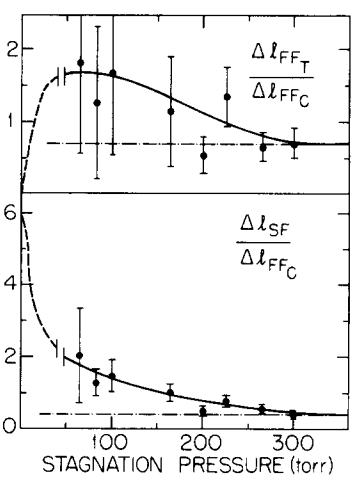

FIG. 8. Evidence of incomplete V–V relaxation. Ratio of increases in rms amplitudes as functions of stagnation pressure. All runs were made with nozzle 2, 20 W $P(20)$ line at $x_L = 0.1$ mm. Values of the amplitude ratios at 0 Torr correspond to a pure ν_3 mode. Solid lines are drawn through experimental points. Dashed lines connect experimental points to the low pressure limits. Dash–dotted lines represent ratios for a vibrational Boltzmann distribution. Error bars are $\pm 1\sigma_{LS}$ for a representative single plate.

IV. DISCUSSION

A. Design of experiment

The new nozzle designs, which made the present series of experiments feasible, successfully remedied the chief source of trouble in the previous study.[5] This was the direct heating of the nozzle and, with it, the gas flowing through it during irradiation by the laser beam. With the new nozzles the intense part of the laser beam could be brought into direct contact with the nozzle for short periods without inducing a significant temperature rise. This permitted investigation with much higher power densities at the nozzle tip and made it possible to detect the V-T/R relaxation, which had been obscured in previous work. The new nozzles, however, introduced an optical complication to be discussed later.

Electron diffraction probing of the irradiated molecules provided a test of the proposed model of absorption kinetics, gave information about V–V and V-T/R relaxation rates in greatly excited samples, and afforded a measure of the distribution of excitation among the molecules sampled by the electron beam as discussed in the following sections.

B. Distribution of excitation

In the previous study,[5] a procedure was described for analyzing whether the diffraction intensities were better described in terms of a single population of molecules existing

in a Boltzmann distribution of excitation at a common vibrational temperature or in terms of a mixture of a cool and a vibrationally hot population. It had been found for samples excited thermally by a hot nozzle or by direct laser pumping to modest excitations ($\langle n \rangle \leqslant 2$ photons/molecule) that intensities were accounted for by a single, moderately hot population. In the present work, however, three plates corresponding to higher excitations ($\langle n \rangle \geqslant 3.5$ photons/molecules) were analyzed and found to be represented significantly better (fit improved 25%) by a cool and a very hot population. The best fit was obtained when the excited molecules comprised 62% of the total population. The meaning of this is not clear. A high collision rate is required for molecules to absorb many photons, and molecules in the outer streamlines of effluent gas experience fewer collisions on their way to the electron beam than do those in the inner streamlines, as shown in Table III. Presumably, then, molecules in different streamlines absorb at somewhat different rates. This condition was also present in experiments with smaller excitation, however, and except for the possibility of nonuniform distribution of laser intensity caused, somehow, by reflections from the polished nozzle, the uniformity of irradiation in the various experiments was not greatly different. In a different study[12] at a lower pressure of SF_6 (2 Torr), populations of hot and cold molecules had been observed together immediately after excitation. Within 3 μs, however, the sample had relaxed to a Boltzmann distribution. In the present experiments, there is a 2 μs interval between excitation and measurement but half of the collisions take place in the first 0.2 μs and most of the rest occur soon after in the supersonic expansion.

C. V–V relaxation

As is evident in Fig. 7, the V–V relaxation is essentially complete in most of the experiments carried out. When stagnation pressures were decreased below about 200 Torr, however, and total collisions (averaged over streamlines) fell below 150, evidence for incomplete V–V relaxation began to appear. This was manifested in the pattern of rms amplitudes of vibration represented in Fig. 8. To spectroscopists accustomed to V–V relaxation experiments carried out at pressures well below 1 Torr, stagnation pressures of 65–200 Torr may seem excessive for such observations. Some perspective on this can be acquired from the gas kinetic calculations in Table II listing the total collisions experienced by molecules, emerging in various streamlines from the nozzle, during their flight to the probing electron beam 0.7 mm away. (Very few additional collisions occur subsequently in the rapidly expanding jet.) Of the collisions listed, half occur in the first 0.003 cm of trajectory before the molecules have been subjected to 0.2 μs exposure to the laser beam, and the remainder occur soon after at progressively lower translational temperatures. Moreover, approximately half of the absorption takes place after half of the collisions have occurred, according to model calculations. In order of magnitude we shall take for the collision number Z_{vv} for V–V relaxation half the total collisions at the pressure associated with relaxation into bending modes. At P(stagn) $\approx$ 100 Torr, this suggests $Z_{vv} \approx 30$ collisions, a value within a factor of 3 of that established by Knudtson and Flynn[12] for relaxation into the ν_4 bending mode.

Whether our larger value is genuinely larger because of the substantially lower mean temperatures of relaxation or whether it simply reflects the imprecision evident in Fig. 8 is uncertain. More definite is that relaxation from ν_3 to the other stretching modes is much faster, and has already occurred at the lowest pressures and shortest times analyzed in our experiment. If molecules probed by our electron beam had remained in the pumped ν_3 mode, the amplitude ratios would have been these shown by the dashed curve intercepts at zero pressure in Fig. 8. A very much faster V–V relaxation away from ν_3 than the overall V–V rate established by Knudston and Flynn[13] is consistent with the infrared double resonance interpretations of Steinfeld *et al.*,[14] Frankel,[15] and Deutsch and Brueck.[16] A crude analysis of the three independent rms amplitudes measured at various pressures in terms of mean excitation of pumped mode, of other stretch modes, and of bending modes is given in Table III. Its basis is sketched in the Appendix.

D. V-T/R relaxation

At the higher pressures studied the heat liberated by V-T/R processes begins to alter the gas dynamics of expansion measurably. Jet densities ρ reaching the electron beam are significantly lower in comparison with those (ρ_c) of unpumped jets, and this is reflected in exposures E of the dif-

TABLE II. Total number of molecular collisions experienced from nozzle tip to electron beam in the streamlines of a gas jet of SF_6 issuing from nozzle 2 as a function of stagnation pressure.[a]

Stagnation pressure (Torr)	Streamline number of ten equispaced lines, 1 innermost.				
	1	4	7	10	$\bar{Z}$[b]
65	40	37	28	9	30
100	73	68	52	17	55
200	204	190	145	45	155
300	336	314	240	79	255
600	740	695	535	170	565
900	1150	1075	825	265	875
1200	1545	1445	1115	355	1175

[a] Calculated on hard-sphere basis, 5.5 Å collision diameter, J. O. Hirschfelder, C. F. Curtiss, and R. B. Bird, *Molecular Theory of Gases* (Wiley, New York, 1954).
[b] $\bar{Z}$ is the collision number averaged over streamlines as by a probing electron beam.

TABLE III. Estimation of the distribution of vibrational excitation among pumped (p), other stretching (s), and bending (b) modes of SF_6 expressed as mean vibrational quantum numbers v inferred from observed mean square amplitudes.

	1σ uncert.	Stagnation pressure (Torr) 65	82	100	165	200	265	300
$10^4\Delta(l^2_{FF_T})$ in Å^2	1.8	2.86	2.41	2.98	3.07	4.13	6.17	10.00
$10^4\Delta(l^2_{SF})$ in Å^2	0.4	1.27	1.91	2.10	2.02	3.35	4.34	4.86
$10^4\Delta(l^2_{FF_c})$ in Å^2	0.5	0.87	2.10	2.02	2.80	9.28	10.20	18.00
v_s[a]	0.03	0.06	0.05	0.06	0.06	0.07	0.12	0.19
v_p[b]	0.04	0.03	0.06	0.06	0.06	0.11	0.14	0.12
v_b[c]	0.03	0.00	0.03	0.02	0.04	0.18	0.18	0.34
$\langle n\rangle$[d]	0.3	0.2	0.4	0.4	0.5	1.3	1.5	2.4
$\langle n\rangle^*$[e]	0.15	0.1	0.2	0.2	0.3	1.1	1.3	2.3

[a] $\Delta(l^2_{FF_T}) = 52.2\,v_s$.
[b] $\Delta(l^2_{SF}) = 13.0\,v_s + 20.6\,v_p$.
[c] $\Delta(l^2_{FF_c}) = 12.3\,v_s + 4.3\,v_p + 44.6\,V_b$.
[d] $\langle n\rangle = [v_s(2058) + v_p(2844) + v_b(4464)]/948$ is the estimated number of photons absorbed per molecule.
[e] $\langle n\rangle^*$ would be the apparent number of photons absorbed if inferred solely from the increase in FF_{cis} amplitude, assuming a thermal distribution.

fraction plates. Exposures are directly proportional to the integrated density along the electron beam. Despite the 7% rms noise in exposures there is a clear trend of E/E_c downward to about 0.84 as pressure and excitation increase. It is possible to estimate the order of magnitude of heat transferred during relaxation by several approaches, the simplest of which is as follows. The effect of the greater vibrational heat evolved by the pumped molecules in comparison with the control during the expansion is simulated by a greater effective heat capacity and, therefore, smaller effective γ. In free jet expansions the divergence angle ϕ characterizing the expansion increases in a known way as γ decreases[17] and the additional velocity imparted, which further diminishes the jet density, is readily calculated. At the highest stagnation pressures, experiments indicate that approximately one-tenth of the absorbed radiant energy is transferred to translation/rotation energy in the course of 1200 collisions (see Table II). In the present experiments the ensemble is enormously hotter, vibrationally and quickly becomes much cooler, translationally, than in the more conventional, more precise procedures[13,18,19] to measure V-T/R relaxation.

E. Test of model of pumping kinetics

It is well to keep in mind that the kinetics of pumping of supersonic jets involves not only the imperfectly understood interaction of radiation with an inhomogeneous ensemble of molecules but also the complex dynamics of the supersonic expansion itself in a seldom studied region. Nevertheless, a model (Appendix A) was devised[6] for the calculation of $\langle n\rangle$ as a function of power density distribution, nozzle dimensions, and gas stagnation pressure with few empirical parameters. One of these, b, characterizing the jet breadth, was measured experimentally[4] in unirradiated jets. The others (h_1 expressing the competition between molecule–molecule and photon-molecule collision rates, and n_p and n_w, two pure numbers expected to be of the order of unity) were estimated from Quigley's measured cross sections[20] in static systems of SF_6 and Xe. Encouraged by the model's semiquantitative success[3] in accounting for two series of experiments[2,5] carried out under widely differing conditions by different techniques, we designed the present series of experiments to test its principal features. Unfortunately, an unanticipated optical imperfection was recognized near the end of the work which, as will be explained, somewhat marred the absolute values of $\langle n\rangle$ derived but still allowed useful measures of the dependence of $\langle n\rangle$ upon wavelength, power, nozzle geometry, and gas density. Static (low power) cross sections as a function of frequency and temperature used in model calculations were taken from Nowak and Lyman.[21]

Observed excitation spectra illustrated in Fig. 1 for all three rms amplitudes at two power densities display increasing red shifts with increasing excitation in qualitative agreement with expectations. Calculated excitation spectra are compared in Fig. 10 with experimental points deduced from the *cis* amplitudes. Although the model $\langle n\rangle$ are of the correct magnitude, they display a smaller red shift than is observed. Observed increases in bond length accompanying excitation (Fig. 2) agree within ten thousandths of an angstrom with increases in thermally heated SF_6[11] at the same vibrational temperatures. The nonlinear dependence of absorption upon incident power is represented fairly well by the calculated curve in Fig. 3. Increasing power leads to saturation unless the collision rate is increased proportionately to fill the hole burnt in the small (0.3%)[22] population of states capable of absorbing the incident wavelength. Varying the collision rate by varying the sample reservoir pressure, then, is expected to have a marked effect on absorption. This is observed and well represented by the model calculations depicted in Fig. 4.

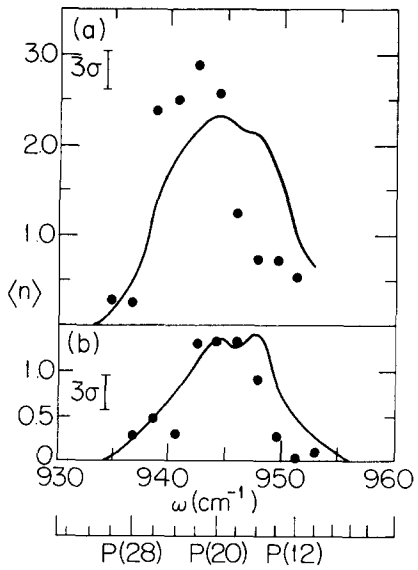

FIG. 10. Observed (points) and calculated (solid lines) excitations $\langle n \rangle$ as a function of pumping frequency for conditions of Fig. 1. Nozzle 2, upper curve; nozzle 1, lower. Calculation model of Ref. 6.

Another aspect of the density-power relation is manifested in the variation of absorption with nozzle dimensions for a given throughput of gas. Nozzle 3 was fashioned to have an inner diameter threefold larger than that of nozzle 1. At throughputs of 0.36 Torr ℓ/s and common power densities from a 20 W beam, gas from nozzle 3 was observed to absorb 0.68 times the number of quanta per molecule as gas from nozzle 1. Model calculations yielded the fraction 0.70. Here it is worth pointing out that the gas density at the nozzle tip of the larger nozzle was an order of magnitude lower than that of the smaller nozzle. What prevented $\langle n \rangle$ from being much smaller, then, was the greater length over which collisions were maintained.

Less convincing results of the model calculations appear in the excitation profiles in Fig. 5 illustrating the variation of absorption as the laser beam is translated along the jet axis. Here, ideally, if the focused laser spot were narrow compared with the jet collisional rate profile, would be mapped the jet absorption efficiency. If the laser spot were broad compared with the distance over which the jet absorbed, the curve would reproduce, instead, the power density profile of the laser beam. In fact, the measured power density profile ($\sigma_L = 0.15$ mm) is intermediate and *broader* near its peak than the curve of Fig. 5. The simplest way to account for the narrowness of the observed response curve and its greater than expected maximum value is to postulate that radiation reflected from the broad,[23] polished, not quite flat nozzle surface may be coherently superposed upon the direct radiation to give interference features narrower than, and in places substantially more intense than, the original intensity profile. The mixing of two equally intense beams produces maxima with fourfold greater intensity than possessed by either beam alone. That this unanticipated effect, a major potential source of the irregularities in the data points plotted in the figures, is plausible is supported by the following evidence. Without an interference effect a peak as sharp as the observed peak *could not result* (given $\sigma_L = 0.15$ mm) even if the absorption region were vanishingly narrow. Model calculations of interference patterns produced by reflection at a grazing angle can account for interference regions narrower than the incident beam. Furthermore, the profile calculated with the model of paper III[6] using as input the published experimental conditions of Coulter *et al.*[2] gave a quantitatively accurate representation of their profile (Fig. 3 of Ref. 2). The relative breadths of their nozzle orifice and laser beam were similar to ours but their optical system apparently avoided disturbing reflections.

After reviewing the performance of the computational model, it is appropriate to recall some of the more important simplifications it adopts. At large pressures V-T/R relaxation, which has not been but could be incorporated into the model, begins to be felt. Its influence would become crucial in calculations attempting to simulate experiments irradiating gas flowing through a transparent nozzle.[24] Another consideration not routinely taken into account in the model is the attenuation of the laser beam before it reaches the streamlines sampled by the electron beam. Effects of this absorption by gas molecules are small until pressures attain the greatest values studied in our experiment. At such high gas densities the attenuation can reach 50%. The corresponding percentage correction in calculated $\langle n \rangle$ for the $P(20)$ line at normal power is less than 20%, however. At the high vibrational temperatures attained, increased absorption depresses the cross section, flattening the $\langle n(W) \rangle$ response curve.

Another oversimplification of the model is the omission of any correction for the great disparity between rotational and vibrational temperatures. In principle, if the assignments of all important transitions were known, including those at substantial vibrational excitation, correction factors could be computed. In practice it was hypothesized that the vibrational temperature is more important than the rotational temperature and static cross sections σ_s were, accordingly, based on vibrational temperature. The dropoff of cross section with decreasing collisional rate (which is related to T/R temperature) *is* built into the model. Experiments to date have not revealed a serious deficiency due to the simplification. A theoretical investigation of cross section examining in some detail the consequences of disparity between rotational and vibrational temperatures found comparatively modest effects of changes in rotational temperatures.[25]

Too little information is available to check the simplified gas dynamics and modeling of absorption kinetics in a region of rapidly dropping temperature and gas density. Yet, despite its approximations (most of which are amenable to improvement should the need arise), the model of collisionally assisted laser pumping of supersonic jets seems to have captured a substantial element of truth. In an elementary way it has given a satisfactory account of the different tests it was put to, for the most part within the experimental error associated with the unstable power density profile. Accordingly, it may prove helpful in designing molecular beam experiments in which a high intensity, vibrationally excited beam is desired whose excitation can be modulated at will.

ACKNOWLEDGMENTS

This research was supported by the National Science Foundation under grant no. CHE-7926480. We thank Dr.

Edward Valente and Mr. Anding Jin for their considerable assistance. We gratefully acknowledge a generous allocation of computing time from the University of Michigan Computing Center.

APPENDIX

1. Kinetics of laser pumping

In the following is sketched the approach to a treatment of infrared absorption by a supersonic jet. A detailed account is given elsewhere.[6,7] From the definition of σ, the molecular cross section for absorption, can be written

$$d\langle n(\mathbf{r})\rangle = \frac{\sigma w(\mathbf{r})dx}{v(\mathbf{r})h\nu\cos\theta} \tag{A1}$$

for the number of photons/molecule absorbed in a given streamline passing through r at an angle θ to the jet axis (x axis) while the molecule is advancing from x to $x+dx$ with speed $v(\mathbf{r})$ through a power density $W(\mathbf{r})$. Cross section σ is diminished from the "static" value $\sigma_s(T_v,\nu)$, measured at vibrational temperature T_v with a weak incident beam, to the extent that collisions fail to replenish pertinent states (susceptible of pumping) as fast as such states are removed by absorption. A plausible relation

$$\sigma = \sigma_s(T_v,\nu)/\left[1+(P_{1/2}/P_{\text{eff}})^{n_p}\right] \tag{A2}$$

was found to represent prior data[20] reasonably well if $P_{1/2}$ is taken as $h_1 W^{n_w}$ with constants n_p and n_w near unity at 0.8 and 0.7, respectively. Proportionality constant h_1 was proposed to be 0.13 Torr $(\text{W/cm}^2)^{-0.7}$ for SF_6–SF_6 collisions. The effective pressure is simply the actual pressure if the gas is at the temperature T_N of the nozzle tip but is assumed to scale as (hard sphere) collision frequency, or

$$P_{\text{eff}} = (T_t/T_N)^{1/2}(\rho/\rho_N)P_N \tag{A3}$$

at the lower translational temperatures T_t and densities ρ encountered in the jet where collision rates are slowed. Procedures to calculate the velocities, densities, temperatures, angles θ, and power densities in the various streamlines as functions of x are presented in paper III[6] and a thesis.[7]

2. Inference of V–V relaxation

Entirely different features of diffracted intensities give a measure of V–V than of V-T/R relaxation. This information is latent within the pattern of amplitudes of vibration. For example, an ensemble excited only in the ν_3 pumped mode would exhibit an appreciable increase in amplitude of the SF pair, a modest increase for the FF(*cis*) pair, and no increase for the FF_{trans} pair. As energy relaxes to the other stretch modes, the FF_{trans} amplitude shows a decided excitation. When bends acquire their equilibrium share, the FF(*cis*) amplitude rises substantially at some cost to the bond-stretching amplitudes. With only three types of atom-pairs providing data, however, too little information is available to determine the complete distribution of energy among the six types of normal modes. Nevertheless, by making plausible assumptions it is possible to assign rough values to excitation in (a) the pumped mode, in (b) the other stretching modes, and in (c) the bending modes. For sake of simplicity we took each mode in a given one of the classes (b) or (c) to have the same average quantum number and, applying a computational procedure given elsewhere,[7,26] obtained the apportionments of energy listed in Table III.

[1] M. M. Arvedson and D. A. Kohl, Chem. Phys. Lett. **64**, 119 (1979).
[2] D. R. Coulter, F. B. Grabiner, L. M. Casson, G. W. Flynn, and R. B. Bernstein, J. Chem. Phys. **73**, 281 (1980).
[3] L. S. Bartell, S. R. Goates, and M. A. Kacner, Chem. Phys. Lett. **76**, 245 (1980).
[4] L. S. Bartell, M. A. Kacner, and S. R. Goates, J. Chem. Phys. **75**, 2730 (1981).
[5] L. S. Bartell, M. A. Kacner, and S. R. Goates, J. Chem. Phys. **75**, 2736 (1981).
[6] L. S. Bartell and M. A. Kacner, J. Phys. Chem. (in press).
[7] M. A. Kacner, Ph.D. thesis, University of Michigan, 1983.
[8] See AIP document No. PAPS JCPSA-**81**-280-18 for 18 pages of experimental conditions for all diffraction plates, analyses of the plates, representative experimental intensities, and the nozzles as a function of stagnation pressure. Order by PAPS number and journal reference from American Institute of Physics, Physics Auxilliary Publication Service, 335 E. 45 St., New York, NY 10017. The price is $1.50 for each microfiche (98 pages) or $5 for photocopies of up to 30 pages and $0.15 for each page over 30 pages. Airmail is additional. Make checks payable to the American Institute of Physics.
[9] S. J. Cyvin, *Molecular Vibrations and Mean-Square Amplitudes* (Elsevier, Amsterdam, 1968).
[10] B. R. Miller and L. S. Bartell, J. Chem. Phys. **72**, 800 (1981).
[11] S. R. Goates and L. S. Bartell, J. Chem. Phys. **77**, 1866, 1874 (1982); J. Stanton and L. S. Bartell (unpublished data).
[12] V. N. Bagratashvili, Yu. G. Vainer, V. S. Dolzhikov, S. F. Kol'yakov, V. S. Letokhov, A. A. Makarov, L. P. Malyavkin, E. A. Ryabov, E. G. Sil'kis, and V. D. Titov, Sov. Phys. JETP **53**, 512 (1981).
[13] J. T. Knudtson and G. W. Flynn, J. Chem. Phys. **58**, 1467 (1973).
[14] J. I. Steinfeld, I. Burak, D. G. Sutton, and A. V. Nowak, J. Chem. Phys. **52**, 5421 (1970).
[15] D. S. Frankel, J. Chem. Phys. **65**, 1696 (1976).
[16] T. F. Deutsch and S. P. J. Brueck, J. Chem. Phys. **70**, 2063 (1979).
[17] See, for example, H. Ashkenas and F. S. Sherman, *Rarified Gas Dynamics, Fourth Symposium*, edited by J. M. de Leeuw (Academic, New York, 1966), Vol. II, p. 84.
[18] C. L. O'Connor, J. Acoust. Soc. Am. **26**, 361 (1954).
[19] R. Holmes and M. A. Stott, J. Sci. Instrum. **44**, 136 (1967).
[20] G. P. Quigley, Opt. Lett. **3**, 106 (1978).
[21] A. V. Nowak and J. L. Lyman, J. Quant. Spectrosc. Radiat. Transfer **15**, 945 (1975).
[22] I. Burak, J. I. Steinfeld, and D. G. Sutton, J. Quant. Spectrosc. Radiat. Transfer **9**, 959 (1969); C. K. N. Patel and R. E. Slusher, Phys. Rev. Lett. **20**, 1087 (1968).
[23] Inasmuch as the absorption takes place in the first nozzle diameter or so of the jet flow, it is only necessary that the breadth of the polished region responsible for reflections be large compared with the 10^2 μm span of the jet orifice.
[24] M. I. Lester, D. R. Coulter, L. M. Casson, G. W. Flynn, and R. B. Bernstein, J. Phys. Chem. **85**, 751 (1981).
[25] R. S. Taylor, T. A. Znotins, E. A. Ballisk, and B. K. Garside, J. Appl. Phys. **48**, 4435 (1977).
[26] M. A. Kacner and L. S. Bartell, J. Chem. Phys. **71**, 192 (1979).